Characteristics of populations and gains in neon-like argon (Ar IX)

Dong-Eon Kim[a)]
Department of Physics, Pohang University of Science and Technology, Pohang, 790-784, Korea

Dae-Soung Kim
Department of Office Automation, Youngwol Institute of Technology, Youngwol, Kangwon-Do 230-800, Korea

Albert L. Osterheld
Lawrence Livermore National Laboratory, L-41, P. O. Box 808, Livermore, California 94551

(Received 21 January 1998; accepted for publication 20 August 1998)

The characteristics of the populations and gain coefficients in Ne-like Ar have been investigated considering the 37 levels of the $2p^6$, $2p^5 3s$, $2p^5 3p$, $2p^5 3d$, $2s2p^6 3s$, $2s2p^6 3p$, and $2s2p^6 3d$ configurations. It was found that large gains on the $3p\ ^1S_0-3s\ ^1P_1$, $3p\ ^3P_2-3s\ ^1P_1$, and $3p\ ^3D_2-3s\ ^3P_1$ transitions are formed for the density between 10^{18} and 10^{19} cm^{-3}. The effect of the opacities of the $2p\ ^1S_0-3s\ ^3P_1$, $2p\ ^1S_0-3s\ ^1P_1$, $2p\ ^1S_0-3d\ ^3D_1$, $2p\ ^1S_0-3d\ ^1P_1$, and $2p\ ^1S_0-2s3p\ ^1P_1$ transitions becomes important for a density higher than 10^{18} cm^{-3} and even increases the gain on the $3p\ ^1S_0-3s\ ^1P_1$ transition for the opacity of the $2p\ ^1S_0-3s\ ^1P_1$ transition of up to 2. © *1998 American Institute of Physics.* [S0021-8979(98)02423-2]

I. INTRODUCTION

Since Zherikhin *et al.*[1] recognized that the populations of some levels in the $2p^5 3p$ configuration can be larger than those in the $2p^5 3s$ configuration for proper electron densities and temperatures, the x-ray laser schemes using transitions between the $2p^k 3p$ and $2p^k 3s$ configurations ($0 \leqslant k < 6$) in ionic systems have been studied both theoretically and experimentally.[2–4] Palumbo and Elton[5] predicted the results of gains on the $3s-3p$ transitions in C-like ions. Vinogradov and Shlyaptsev[6] have shown that the steady-state population inversions for a number of ions between Mg III and Fe XVII can be found. Feldman *et al.*[7] have done the calculations for Be-like, B-like and Ne-like ionic systems, showing that gains could be produced in transitions between the $2p^k 3s$ and $2p^k 3p$ configurations. Rosen *et al.*[8] theoretically predicted the integrated gains on several transitions in Ne-like Se. Experiments using laser-produced plasmas have demonstrated the amplification of expected transitions in Ne-like ions.[2–4,9] In recent years, Rocca and co-workers[10] has reported the observation of soft-x-ray amplification and saturation of the $J=0-1$ transition in Ne-like Ar using a fast capillary discharge. The soft x-ray amplification of the $J=0-1$ transitions has also been demonstrated in other low-Z Ne-like ions such as Ti,[11–13] Cr, Mn,[12] Fe,[12,14] Co, Ni, Cu, and Zn.[14] These works have motivated us to study the gain characteristics of transitions between the $2p^5 3s$ and $2p^5 3p$ configurations in low-Z Ne-like ions, especially argon ions.

In this work, in order to investigate the characteristics of gains in Ne-like Ar, we have calculated level populations and gains on various transitions, using the collisional-radiative model for electron density between $n_e=10^{16}$ and 10^{20} cm^{-3} and electron temperature of $T_e=50$ and 200 eV. This temperature range has been considered because the abundance of the Ne-like ionization stage is expected to be highest for an electron temperature near a half the ionization potential. The collisional-radiative model used here has been used for analyzing atomic population kinetics in non-local-thermodynamic-equilibrium (non-LTE) plasmas at these electron densities.

In the Sec. II, the model and approach in our simulation are described: i.e., the quasi-steady-state collisional-radiative model, atomic model, and the treatment of the opacity. The simulation results are presented and discussed in the Sec. III.

II. MODEL FOR CALCULATION

The rate equation for the population N_l^i of an excited level l in the ith ionization stage is given by

$$\frac{dN_l^i}{dt}=\sum_u R_{ul}^i N_u^i - n_e I_l^i N_l^i + n_e Q_l^{i+1} N_1^{i+1}, \tag{1}$$

with

$$\begin{aligned} R_{ul}^i &= n_e C_{ul}^e, \quad l>u, \\ &= n_e C_{ul}^d + A_{ul}, \quad l<u, \end{aligned} \tag{2}$$

$$R_{ll}^i = -\sum_{m<l}(n_e C_{lm}^d + A_{lm}) - \sum_{m>l} n_e C_{lm}^e,$$

where n_e is the electron density, $C_{ul}^{e(d)}$ the electron excitation (deexcitation) rate coefficient, and A_{ul} the radiative transition rate from a state u to a state l. The terms I_l^i and Q_l^{i+1} represent the electron collisional-ionization rate coefficient from a level l and the total recombination rate coefficient to the level, respectively.

Since an equilibrium between the excited levels is readily established due to their short lifetimes, the quasi-steady-state approximation has been adopted in our calculation:

a)Electronic mail: kimd@vision.postech.ac.kr

$$\frac{dN_l^i}{dt}=0. \tag{3}$$

Furthermore, the recombination and ionization processes between neighboring ionization stages can be ignored because these processes are negligibly slow compared to the excitation and deexcitation processes within the Ne-like ionization stage under the densities and temperatures of our interest. Then, the level populations in a single ionization stage of interest are determined by the balance of collisional and radiative transitions. In the present calculation the level populations are normalized in such a way that

$$m_l=\frac{N_l^i}{N_I}, \quad \sum_l m_l=1, \tag{4}$$

where N_I is the total population of all the levels considered. The relative level populations are calculated by solving the coupled rate equations Eq. (1) under the conditions of Eqs. (3) and (4). The coupled rate equations can then be rewritten in the matrix form:

$$\begin{pmatrix} m_1 \\ m_2 \\ m_3 \\ \vdots \\ m_n \end{pmatrix} = \begin{pmatrix} 1 & 1 & 1 & \cdots & 1 \\ R_{21} & R_{22} & R_{23} & \cdots & R_{2n} \\ R_{31} & R_{32} & R_{33} & \cdots & R_{3n} \\ \vdots & \vdots & \vdots & \ddots & \vdots \\ R_{n1} & R_{n2} & R_{n3} & \cdots & R_{nn} \end{pmatrix}^{-1} \begin{pmatrix} 1 \\ 0 \\ 0 \\ \vdots \\ 0 \end{pmatrix}. \tag{5}$$

In this study, the 37 levels of the $2p^6$, $2p^5 3s$, $2p^5 3p$, $2p^5 3d$, $2s2p^6 3s$, $2s2p^6 3p$, and $2s2p^6 3d$ configurations in Ne-like Ar have been considered. All the radiative and collisional processes between the 37 levels have been taken into account. The necessary atomic data were obtained from the Hebrew University-Lawrence Livermore Atomic Code package (HULLAC). In the atomic structure calculation, the wavefunctions, energy levels, and all the important radiative decay rates were obtained from a relativistic configuration interaction treatment based on a parametric potential model.[15] Electron impact excitation cross sections were calculated in the semirelativistic, distorted-wave approximation using the techniques of Ref. 16. In this approach, the cross section is factorized into a radial part involving wavefunctions only, and an angular factor depending only on the target states. The semirelativistic approximation treats the continuum electron nonrelativistically, while retaining a fully relativistic treatment of the bound electrons. The cross sections were averaged over a Maxwellian velocity distribution with a temperature T_e to obtain excitation rate coefficients. The electron excitation rate coefficients were approximated by the five-parameter fit:[17]

$$C_{lu}^e=\langle \sigma v \rangle = 1.58\times 10^{-5}\frac{p(b_{lu})}{b_{lu}\gamma}e^{-b_{lu}} \text{ cm}^3/\text{s}, \tag{6}$$

where

$$b_{lu}=\frac{E_{lu}}{\gamma}, \tag{7}$$

and

$$\ln p(b_{lu})=c_0+c_1\ln b_{lu}+c_2\ln^2 b_{lu}+c_3\ln^3 b_{lu}, \tag{8}$$

where E_{lu} is the transition energy (in eV) and $\gamma=T_e$ the electron temperature (in eV). The deexcitation rate coefficient is obtained using the detailed-balance relation

$$C_{ul}^d=\frac{g_l}{g_u}e^{b_{lu}}C_{lu}^e. \tag{9}$$

For a Doppler-broadened spectral line, the gain coefficient on a radiative transition between an upper level u and a lower level l is given by

$$G=\frac{1}{8\pi}\left(\frac{M}{2\pi kT_{\text{ion}}}\right)^{1/2}A_{ul}\lambda_{ul}^3 g_u\left(\frac{N_u}{g_u}-\frac{N_l}{g_l}\right) = \sigma_{\text{gain}} g_u\left(\frac{N_u}{g_u}-\frac{N_l}{g_l}\right), \tag{10}$$

where M is the atomic mass of the ion, k the Boltzmann constant, T_{ion} the ion temperature, λ_{ul} the wavelength of the transition, g_u and g_l the statistical weights of the levels, N_u, N_l the population of the levels u and l, respectively, and σ_{gain} the gain cross section. Ion temperature T_{ion} were chosen to be approximately equal to electron temperature T_e; however, T_{ion} may be smaller than T_e.

Using the relative populations, Eq. (10) can be rewritten as follows:

$$G_{ul}/N_I=9.98\times 10^{-32}A_{ul}\lambda_{ul}^3\frac{1}{T_e^{1/2}}g_u\left(\frac{m_u}{g_u}-\frac{m_l}{g_l}\right) \text{ cm}^{-4}, \tag{11}$$

where λ is given in angstrom, T_e in eV. The right-hand side of Eq. (11) consists of terms only related to Ne-like Ar. Hence, it represents inherent characteristics of gain on a transition in Ne-like Ar for a given electron temperature and density.

A rapid radiative decay of the lower level is crucial to the formation of the population inversion between the two levels. Thus, the radiation from the lower level should freely escape from a plasma. In other words, the plasma must be optically thin to the transition from the lower level, at least in the transverse direction. We have also investigated the opacity effect on gains. The opacity τ on a radiative transition between the levels l and m is defined by

$$\tau_{lm}=k_{lm}(\lambda)L, \tag{12}$$

where L is the effective length of the plasma medium and $k_{lm}(\lambda)$ the absorption coefficient, which is given by

$$k_{lm}(\lambda_{lm})=\frac{e^2 f_{lm}}{m_e c^2}\left(\frac{\pi Mc^2}{2kT_{ion}}\right)^{1/2}N_l\lambda_{lm}, \tag{13}$$

where f_{lm} is the absorption oscillator strength between the levels l and m, m_e the electron mass, and e the electron charge. The opacity has the effect of increasing the population of the upper level involved. High opacity on the resonance transitions between the $2p^6$ and $2p^5 3s$ configurations eventually results in the increase of the level populations in the $2p^5 3s$ configuration, leading to the decrease of gains on the transitions between the $2p^5 3s$ and $2p^5 3p$ configurations.

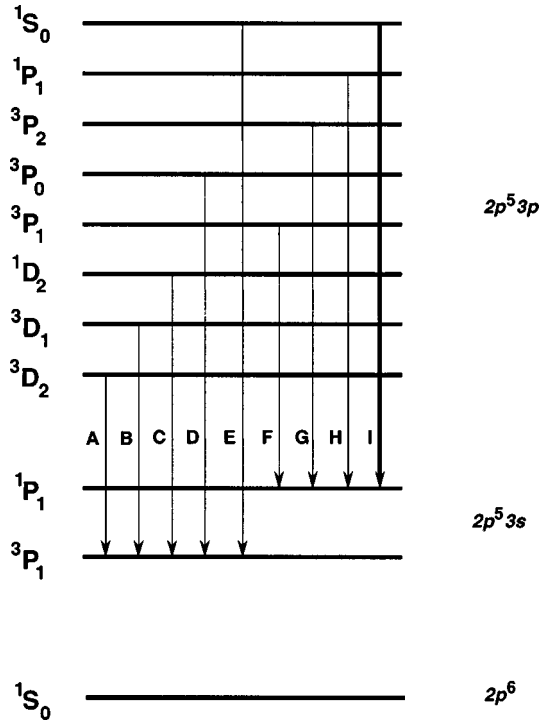

FIG. 1. A schematic diagram of several energy levels under interest in Ne-like Ar (not to scale). The $J=0-1$ transition (I) was observed to have gain and be strongly amplified at proper conditions (Ref. 10).

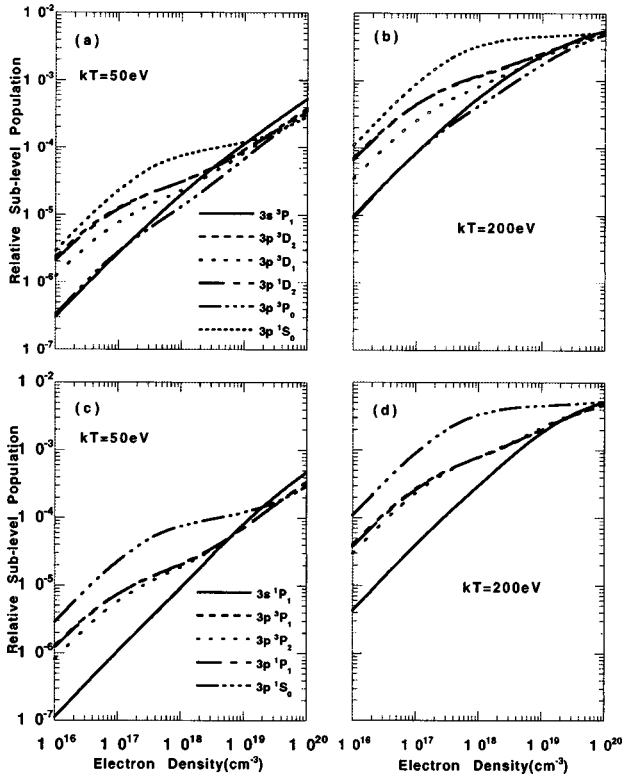

FIG. 2. Relative sublevel populations as a function of electron density for given temperatures: (a) and (c) for $T_e=50$ eV; (b) and (d) for $T_e=200$ eV.

The escape probability method used in our calculation approximates this by the effective reduction of the radiative decay rates. In our case, the radiative decay rate of a relevant transition was replaced by the effective rate given by $E(\tau)A$, where $E(\tau)$ is the escape probability for a given τ and A the original radiative transition rate. For the escape probability $E(\tau)$, we have used the following polynomial fit to tabulated values of $E(\tau)$ calculated by Zemansky:[18]

for $0<\tau\leqslant 4.5$,

$$E(\tau)=0.999003-0.697745\tau+0.266529\tau^2 -0.061906\tau^3+0.008106\tau^4-0.000453\tau^5, \quad (14)$$

and for $\tau>4.5$,

$$E(\tau)=\frac{1}{\tau\sqrt{\pi \ln \tau}}. \quad (15)$$

III. RESULTS AND DISCUSSION

The relative sublevel populations (m_i/g_i) have been calculated by solving the 37 coupled rate equations given by Eq. (5). The gains have then been calculated for the following transitions between the $2s^2 2p^5 3p$ and $2s^2 2p^5 3s$ levels that have large radiative transition rates (see Fig. 1):

(A) $2p^5 3p\ ^3D_2 \rightarrow 2p^5 3s\ ^3P_1$,

(B) $2p^5 3p\ ^3D_1 \rightarrow 2p^5 3s\ ^3P_1$,

(C) $2p^5 3p\ ^1D_2 \rightarrow 2p^5 3s\ ^3P_1$,

(D) $2p^5 3p\ ^3P_0 \rightarrow 2p^5 3s\ ^3P_1$,

(E) $2p^5 3p\ ^1S_0 \rightarrow 2p^5 3s\ ^3P_1$,

(F) $2p^5 3p\ ^3P_1 \rightarrow 2p^5 3s\ ^1P_1$,

(G) $2p^5 3p\ ^3P_2 \rightarrow 2p^5 3s\ ^1P_1$,

(H) $2p^5 3p\ ^1P_1 \rightarrow 2p^5 3s\ ^1P_1$,

(I) $2p^5 3p\ ^1S_0 \rightarrow 2p^5 3s\ ^1P_1$,

In Fig. 2, the relative sublevel populations of the relevant levels are presented as functions of electron densities at given two-electron temperatures of 50 and 200 eV. As shown in Fig. 2, the relative sublevel populations grow with the electron density and the temperature due to the increase of collisional excitation rates. For a given temperature, in the region of low electron density, the populations of the $3s\ ^3P_1$ and $^1P_1$ levels are smaller than those of other levels under consideration due to their strong radiative decay; however, in the region of high electron density, the populations become distributed according to Boltzmann distribution because the collisional deexcitation rates exceed the radiative transition rates. Due to the close collisional coupling of the $2p^5 3p\ ^1S_0$ level to the ground level, the level is most largely populated; however, its inversion against the $2p^5 3s\ ^3P_1$ level destroyed around $N_e=10^{19}\,\mathrm{cm}^{-3}$. The density dependence of the population distribution is maintained for temperatures between 50 and 200 eV. The populations of the $2p^5 3p\ ^1P_1$, $^3P_1$, and $^3D_1$ levels are very close to one another as those of the $2p^5 3p\ ^1P_2$ and $^3D_2$ level are due to the balance of radiative decay and collisional processes. The population of the $3p\ ^3P_0$ level is also very close to that of the $3s\ ^3P_1$ level and its population inversion with respect to the $3s\ ^3P_1$ level is destroyed above the middle of $10^{17}\,\mathrm{cm}^{-3}$. This can be

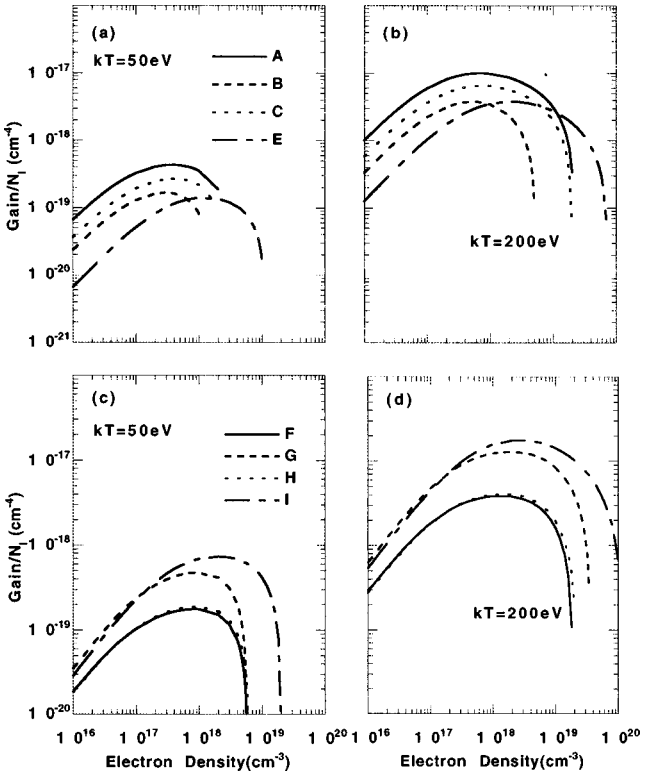

FIG. 3. Gain coefficients per ion density as a function of electron density for given temperatures: (a) and (c) for $T_e=50$ eV; (b) and (d) for $T_e=200$ eV. The designation for the transitions are given in Fig. 1.

explained by the fact that the collisional coupling of the $3p\ ^3P_0$ level to the ground level is not so strong as that of the $3p\ ^1S_0$ level but the $3p\ ^3P_0$ level decays radiatively faster than the $3p\ ^3D_2$, $^1D_2$, and $^3P_1$ levels.

Figure 3 shows the gains on the transitions mentioned above divided by the total Ne-like Ar ion density, Eq. (11). Note that the transitions A, G, and I have potential of high gain. For the electron density below $10^{18}\,\mathrm{cm}^{-3}$, the gains increase with the electron density due to the increase of the collisional excitation rates. The gains reach their maximum in the density region of a few times 10^{17} to a few times 10^{18} cm^{-3} where the collisional deexcitation rates of each transition become comparable to its radiative decay rate. For an electron density higher than about a few times $10^{18}\,\mathrm{cm}^{-3}$ for $T_e=50$ eV and $10^{19}\,\mathrm{cm}^{-3}$ for $T_e=200$ eV, the gains rapidly decrease because the collisional deexcitation rates exceed the radiative decay rates and the population distribution approaches Boltzmann distribution. The gains on the transitions E and I are sustained at higher electron density than on other transitions. Even though the $3p\ ^1S_0-3s\ ^3P_1$ transition (E) shares the $3p\ ^1S_0$ level with the $3p\ ^1S_0-3s\ ^1P_1$ transition (I), its gain is much smaller than that of transition I due to its smaller gain cross section: the gain cross section of transition I is 4.2 times as large as that of the transition E. The larger gain cross sections of the $3p\ ^3P_2-3s\ ^3P_1$ (G) and $3p\ ^3D_2-3s\ ^1P_1$ (A) transitions make their gains comparable to that of the $3p\ ^1S_0-3s\ ^1P_1$ transition (I) even though their upper level populations are several times smaller than that of the $3p\ ^1S_0$ level. Transitions A and G have gain cross sections 3.1 and 4.6 times larger than transition I, respectively.

In Rocca's experiment, the discharge device was operating at 700 mTorr of Ar, which corresponds to the density of about 2.3×10^{16} cm^{-3} at room temperature. The gain on the transition I was observed at the electron density of about or less than 1×10^{19} cm^{-3}. The present calculation shows a gain per particle density on transition I of $1.5\text{–}1.7\times10^{-17}$ cm^{-4} for an electron density of $1\times10^{18}\text{–}1\times10^{19}$ cm^{-3} [Fig. 3(d)] and results in a gain of 0.35–0.4 cm^{-1} for Rocca's experimental conditions, which is in fairly good agreement with the observed value of 0.6 cm^{-1} in that the present calculation did not take into account hydrodynamics. The present calculation also shows a reasonable gain on transition G, the amplification of which was also noticed by Rocca but its gain measurement was not pursued due to the complication of the spectral line being blended with other lines from different ionization stages.

We have also studied the opacity effect. In the calculation, the opacities of the following fast transitions were taken into account: $2p\ ^1S_0-3s\ ^3P_1$, $2p\ ^1S_0-3s\ ^1P_1$, $2p\ ^1S_0-3d\ ^3D_1$, $2p\ ^1S_0-3d\ ^1P_1$, and $2p\ ^1S_0-2s3p\ ^1P_1$. These transitions have larger opacities than other transitions. For a given opacity of a transition α, the opacity of another transition β can be related by

$$\tau_\beta=\tau_\alpha\frac{\lambda_\beta}{\lambda_\alpha}\frac{f_\beta}{f_\alpha}, \tag{16}$$

which only depends on atomic properties. In the calculation, the $2p\ ^1S_0-3s\ ^1P_1$ transition was used as a reference: the values of τ given in Fig. 4 are for the transition. The opacities of the other four transitions were calculated according to Eq. (16). Figure 4 shows the opacity effect on the transitions $3p\ ^1S_0-3s\ ^1P_1$ and $3p\ ^3D_2-3s\ ^3P_1$. Below the electron density of 10^{18} cm^{-3}, the opacity effect is rather small for τ up to 2. The opacity effect becomes important for an electron density larger than 10^{18} cm^{-3} or opacity larger than 4. For a density higher than 10^{18} cm^{-3}, the opacity up to 2 increases the gains. The increase is larger for higher temperature. The opacities in transitions $2p\ ^1S_0-3d\ ^3D_1$, $2p\ ^1S_0-3d\ ^1P_1$, and $2p\ ^1S_0-2s3p\ ^1P_1$ reduce their radiative decay rates, leading to the effective increase of the population of the $3p\ ^1S_0$ level via collisional and radiative cascades. When their opacities are intentionally neglected, the gain in the $3p\ ^1S_0-3s\ ^1P_1$ transition expectedly decreases as shown in Fig. 4(c). The opacity has a larger effect in low temperature than in high temperature: i.e., when the pumping rate is small as in low temperature, even a slight reduction of the decay rate leads to a significant change of the population distribution. It is noted that the $3p\ ^3D_2-3s\ ^3P_2$ transition is less affected than the $3p\ ^1S_0-3s\ ^1P_1$ transition.

IV. CONCLUSION

We have studied the characteristics of the populations of the levels in the $2s^22p^53s$ and $2p^22p^53p$ configurations and the gains on the fast transitions between them. The $3p\ ^3D_2-3s\ ^3P_1$, $3p\ ^3P_2-3s\ ^1P_1$, and $3p\ ^1S_0-3s\ ^1P_1$

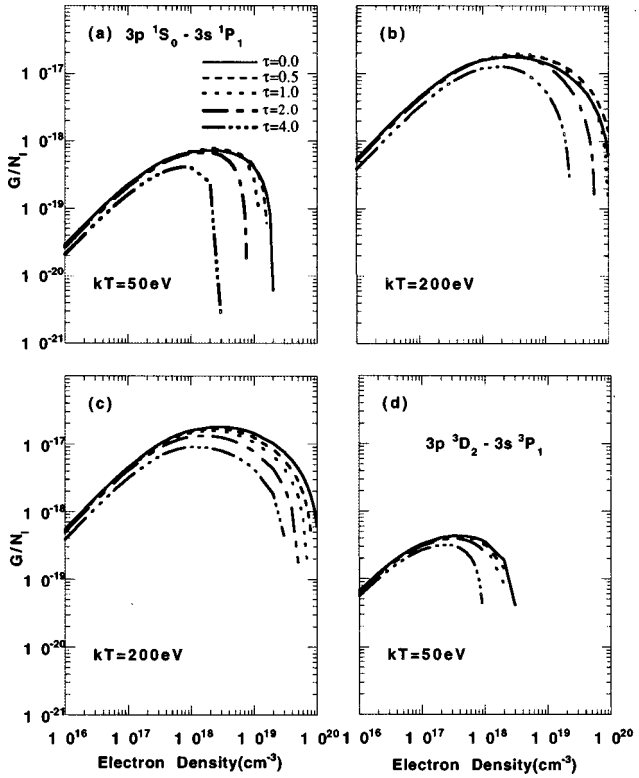

FIG. 4. The opacity effect on gains. The opacities of the $2p\ ^1S_0-3s\ ^3P_1$, $2p\ ^1S_0-3s\ ^1P_1$, $2p\ ^1S_0-3d\ ^3D_1$, $2p\ ^1S_0-3d\ ^1P_1$, and $2p\ ^1S_0-2s3p\ ^1P_1$ transitions are considered. The values of τ are for the $3s\ ^1P_1-2p\ ^1S_0$ transition. (a) The opacity effect on the gain of the $3p\ ^1S_0-3s\ ^1P_1$ transition for $T_e=50$ eV. (b) The same as in (a) but with $T_e=200$ eV. (c) The same as in (b) but in this case the opacities of the $3s\ ^1P_1-2p\ ^1S_0$ and $3s\ ^3P_1-2p\ ^1S_0$ transitions are only taken into account. (d) The opacity effect on the gain of the $3p\ ^3D_2-3s\ ^3P_1$ transition for $T_e=50$ eV.

transitions have large gains. The calculated gain on the $3p\ ^1S_0-3s\ ^1P_1$ transition was found to be in good agreement with the experimental observation. The maximum of the gain on each transition occurs around $N_e=10^{18}$ cm^{-3}. The density dependences of the gains at low and high temperatures are similar.

The effect of the gains due to reabsorption seems negligible if the opacity on the $2p\ ^1S_0-3s\ ^1P_1$ is less than 2 and the electron density is smaller than 10^{18} cm^{-3}. For a higher density than 10^{18} cm^{-3}, the opacity even increases the gains because the reduced radiative decay rates of the transitions between the $2s^22p^53d$, $2s2p^63p$, and $2s^22p^6$ configurations eventually result in the increase of the population of the $3p^1S_0$ level via collisional and radiative cascades.

ACKNOWLEDGMENTS

This work has been supported in part by POSTECH/BSRI special fund, the Basic Science Research Institute Program, Ministry of Education (Project No: BSRI-97-2439), Korea Research Foundation in 1997 and Korea Science Engineering Foundation (Contract No: 951-0205-01702).

[1] A. Zherikhin, K. Koshelev, and V. Letokhov, Sov. J. Quantum Electron. **6**, 82 (1976).
[2] R. C. Elton, *X-ray Laser* (Academic, San Diego, CA, 1990).
[3] B. J. MacGowan *et al.*, J. Appl. Phys. **61**, 5243 (1987).
[4] C. Skinner, Phys. Fluids B **3**, 2420 (1991).
[5] L. J. Palumbo and R. C. Elton, J. Opt. Soc. Am. **67**, 480 (1977).
[6] A. V. Vinogradov and V. N. Shlyaptsev, Sov. J. Quantum Electron. **1**, 754 (1980).
[7] U. Feldman, A. K. Bhatia, and S. Suckewer, J. Appl. Phys. **54**, 2188 (1983); U. Feldman, J. F. Seely, and A. K. Bhaita, *ibid.* **56**, 2475 (1984); U. Feldman, G. A. Doschek, and J. F. Seely, *ibid.* **58**, 2909 (1985).
[8] M. D. Rosen *et al.*, Phys. Rev. Lett. **54**, 106 (1985).
[9] D. L. Matthews *et al.*, Phys. Rev. Lett. **54**, 110 (1985).
[10] J. J. Rocca, V. Shlyaptsev, F. G. Tomasel, O. D. Cortazar, D. Hartshorn, and J. L. A. Chilla, Phys. Rev. Lett. **73**, 2192 (1994); J. J. Rocca, F. G. Tomasel, M. C. Marconi, V. N. Shlyaptsev, J. L. A. Chilla, B. T. Szapiro, and G. Giudice, Phys. Plasmas **2**, 2547 (1995); J. J. Rocca, D. P. Clark, J. L. A. Chilla, and V. N. Shlyaptsev, Phys. Rev. Lett. **77**, 1476 (1996).
[11] T. Boehly, M. Russotto, R. S. Craxton, R. Epstein, and B. Yaakobi, Phys. Rev. A **42**, 6962 (1996).
[12] J. Nilsen, B. J. MacGowan, L. B. Da Silva, and J. C. Moreno, Phys. Rev. A **48**, 4682 (1993).
[13] J. Dunn, A. L. Osterheld, R. Shepherd, W. E. White, V. N. Shlyaptsev, A. B. Bullock, and R. E. Stewart, Proc. SPIE **3156**, 114 (1997).
[14] E. E. Fill, Y. Li, G. Preztler, D. Schogl, J. Steingruber, and J. Nilsen, Phys. Scr. **52**, 158 (1995).
[15] M. Klapisch, J. L. Schwob, B. S. Fraenkel, and J. Oreg, J. Opt. Soc. Am. **67**, 148 (1977).
[16] A. Bar-Shalom, M. Klapisch, and J. Oreg, Phys. Rev. A **38**, 1773 (1988).
[17] S. Dalhed, J. Nilsen, and P. Hagelstein, Phys. Rev. A **33**, 264 (1986).
[18] R. W. P. McWhirter, in *Plasma Diagnostic Techniques*, edited by R. H. Huddlestone and S. I. Leonard (Academic, New York, 1965); M. W. Zemansky, Phys. Rev. **36**, 219 (1930).